PHYSICS OBJECTIVES AND DESIGN OF CIT

D.J. SIGMAR[1], D.B. BATCHELOR[2], G. BATEMAN[3], M.G. BELL[3], B.J. BRAAMS[4], J.N. BROOKS[5], C.Z. CHENG[3], D.R. COHN[1], R.J. GOLDSTON[3], J. HAINES[6], D.N. HILL[7], W.A. HOULBERG[2], C.T. HSU[1], S.C. JARDIN[3], C.E. KESSEL[3], S.S. MEDLEY[3], G.H. NEILSON[2], W.A. PEEBLES[8], F.W. PERKINS[3], R.D. PILLSBURY, Jr.[1], N. POMPHREY[3], M. PORKOLAB[1], W.T. REIERSEN[3], R.O. SAYER[2], J.A. SCHMIDT[3], C.E. SINGER[9], J.C. SINNIS[3], R.D. STAMBAUGH[10], D.P. STOTLER[3], D.J. STRICKLER[2], M. ULRICKSON[3], R.E. WALTZ[10], R.B. WHITE[3], K.M. YOUNG[3]

[1] Massachusetts Institute of Technology,
Cambridge, Massachusetts

[2] Oak Ridge National Laboratory,
Oak Ridge, Tennessee

[3] Plasma Physics Laboratory,
Princeton University,
Princeton, New Jersey

[4] New York University,
New York, N.Y.

[5] Argonne National Laboratory,
Argonne, Illinois

[6] McDonnell Douglas Missile Systems Corporation,
St. Louis, Missouri

[7] Lawrence Livermore National Laboratory,
Livermore, California

[8] University of California,
Los Angeles, California

[9] University of Illinois,
Urbana, Illinois

[10] General Atomics,
San Diego, California

United States of America

Abstract

PHYSICS OBJECTIVES AND DESIGN OF CIT.

The mission of the Compact Ignition Tokamak (CIT) Burning Plasma Experiment is to determine the physics behavior of self-heated fusion plasmas, and to demonstrate the production of substantial amounts of fusion power. In order to achieve this mission with high confidence and minimum cost, CIT is designed as a high-field, LN-cooled, copper-coil tokamak. The confidence of obtaining $Q > 5$, and so being able to fulfill the mission of studying self-heated plasmas, is very high in a device such as CIT, which is projected to obtain $Q \sim 30$ under standard physics assumptions. A class of α-particle collective instabilities potentially capable of causing anomalous losses of fast α's is investigated. Super-Alfvénic ($v_{\parallel\alpha} > v_A$) α's can excite the shear Alfvén gap spectrum of the toroidicity-induced low- and high-n Alfvén eigenmodes, and destabilize ballooning modes and fishbone oscillations. Linear stability results for CIT are given, showing stable and unstable operating windows in $\beta_\alpha - (v_\alpha/v_A)$ space and in $n - T$ space. The generic impact of a fast-α diffusion coefficient, D_α, on fusion performance (Q and $nT\tau_E$) is demonstrated. Full calculations of the effects of disruptions in CIT, including vertical displacement events and associated halo currents, are used to assure that the machine design is consistent with the specification of 10% disruptivity in all modes of operation. By means of a swept divertor configuration, reactor-like surface-average power outflows of 1 MW/m^2 and total fusion power levels up to 500 MW can be safely handled in CIT.

Introduction

The Mission of the Compact Ignition Tokamak (CIT) Burning Plasma Experiment is to "determine the physics behavior of self-heated fusion plasmas, and [to] demonstrate the production of substantial amounts of fusion power." [1] Supporting objectives are to:

1. Demonstrate the production of fusion power in excess of 100 MW, at fusion-reactor-level power density.
2. Determine the confinement physics, operational limits, and α-particle dynamics of self-heated fusion plasmas with α power greater than auxiliary-heating power.
3. Demonstrate heating, fueling, and plasma-handling techniques necessary to produce reactor-level power-density, self-heated fusion plasmas.
4. Optimize plasma performance in the range of $Q = 5$ to ignition, with fusion power up to 500 MW.

These objectives form a set of key tokamak physics issues which can be addressed in a cost-effective manner by a moderate-pulse-length, high-performance DT tokamak. In addition, the information obtained in pursuing these objectives will be highly valuable to the final design and construction of the internal components and external subsystems of

ITER, as well as for ITER's operations phases.

In order to achieve the above objectives with maximum confidence and minimum cost, CIT is designed as a high-field (B_0 = 9 T), relatively compact (R_0 = 2.57 m, a = 0.79 m, κ_{95} = 2), liquid-nitrogen-cooled, copper-coil tokamak device (fig. 1) – in the spirit of the Alcator series of experiments and the LITE design concept [2]. It can be operated in a divertor or inner-wall limiter configuration. All power-handling surfaces are covered with inertially cooled graphite tiles. The vacuum vessel is thick, close-fitting, and highly conductive. The main poloidal-field coils are located outside of the toroidal-field coils, but segmented coils are located within the TF for fast position control. The flat-top time of the device at full field and plasma current (9 T, 11.8 MA) is 10 s, while at 2/3 field and current (6 T, 7.9 MA) the inductive pulse length is 40 s. At fixed Z_{eff} and T_e, this corresponds to the same number of magnetic skin times as 300 s in ITER. Despite its relatively compact design, CIT retains good access for diagnostics and for plasma heating. A full set of profile and fluctuation diagnostics is planned, in addition to diagnostic systems specifically oriented towards measurement of confined and escaping α particles. The initial plasma heating capability will be 20 MW of ICRF power, but access is provided for a significant upgrade of the ICRF system, or for inclusion of ECRF heating power.

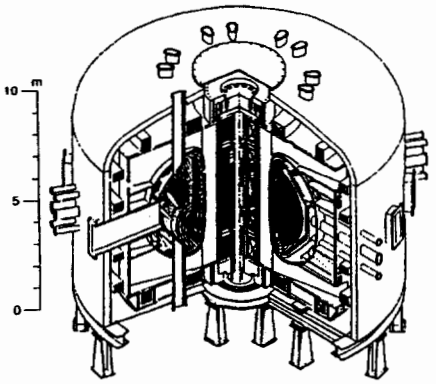

Fig. 1: Cutaway view of the CIT Burning Plasma Experiment. R = 2.57 m, a = 0.79 m, B_T = 9T, κ_{95} = 2.0, I_p = 11.8MA, P_{RF} = 20MW.

The design of the CIT device has evolved since the previous IAEA meeting [3] in the direction of lower field and greater size, in order to reduce both magnet stresses and power loading on the divertor and first wall. At the same time the magnet design has moved away from developmental materials, such as explosively bonded copper-steel laminate and Nitronic-40, towards better-characterized engineering materials, such as high-strength beryllium copper, 316LN stainless steel, and Inconel. Centering and overturning forces in the toroidal field coil are supported in a wedged configuration as before, but instead of employing a 2-sector vacuum vessel, the machine design is now modularized into six sectors, each composed of three toroidal field coils, four segments of fast position-feedback control coils, and a vacuum-vessel segment. This design permits factory construction and internal alignment of each module, and therefore easier and more reliable field assembly and maintenance. The general thrust of the engineering design is towards high performance, simplicity, and robustness.

In this paper we discuss projections for CIT's performance (including uncertainties), and the α-particle physics issues which CIT will address. We also highlight analyses of two key areas of engineering physics in CIT: disruptions and power handling.

Performance Projections

The planned Reference Operating Mode of CIT [1] in many respects falls within the standard operating range of current H-mode tokamaks: $q_{95} \sim 3.2$, $\kappa_{95} \sim 2$, $\beta \sim 2\times10^{-8}$ I/aB_0, $\langle n \rangle \sim 5\times10^{13}$ $I_p/(\pi a^2)$ (all units SI), double-null divertor. The dimensionless parameters $B\tau_E$ ($\omega_c\tau_E$) and $nT\tau_E/B$ ($\beta\omega_c\tau_E$) [4] give physically meaningful measures of the required degree of extrapolation in confinement properties beyond the present tokamak database. In these variables CIT stands midway between JET and ITER, and so represents a relatively modest physics extrapolation, but as a high-field device, CIT still attains $nT\tau_E$ values comparable to ITER's, about 10x those attainable in JET. Our primary reference for projecting the performance of CIT is the ITER89-P scaling relation [5], coupled with a multiplicative factor to take into account the enhanced confinement observed in the H-mode. This approach is justified by the observation that tokamaks as modest as JFT-2M ($a = 0.28$m, $B_T = 1$T) and as powerful as JET ($a = 1.2$ m, $B_T = 3$ T) see rather similar H-mode signatures and confinement enhancements over L-mode. Review of the available data on quasi-steady-state, relatively low q, H-mode performance leads us to believe that enhancement factors, C_τ, in the range of 1.5 – 2.2 should be expected, giving a median C_τ of 1.85. Summing the estimated range of uncertainty in C_τ in quadrature with the uncertainty in L-mode extrapolation to CIT of 15 – 20% [6], we obtain an overall uncertainty in the H-mode confinement projection of about 23%. Future detailed analysis of the recently constructed ITER H-mode database [7], concentrating on quasi-steady-state, low-q operation, should allow refinement of these estimates.

In order to estimate the expected range of performance for CIT, we have employed a Monte-Carlo technique [8] to sample out of a Gaussian distribution of Z_{eff}'s (1.65 ± 0.35), density profile shapes ($n \alpha (1 - \rho^2)^v$, $v = 0.5 \pm 0.5$), and confinement enhancement factors relative to ITER89-P ($C_\tau = 1.85 \pm 0.43$) in order to estimate both the median expected fusion gain of CIT, and its range of uncertainty. Z_{eff} is taken rather low due to the observation that the high-field Alcator tokamaks maintain low Z_{eff} at the high plasma densities and surface power densities accessible at high B_T/R. The density profile shape ranges from flat to parabolic, to take into account the observation that many H-mode plasmas have rather flat density profiles, while, on the other hand, CIT will be equipped with a high-speed (4-5 km/s) deeply-penetrating pellet injector, which may permit significant peaking of the density profile. Recent results on TFTR [9] support the idea that strong central fueling can be used to maintain steady-state peaked density profiles in the H-mode. The temperature profiles are taken to be trapezoidal, with a flat central region extending to $\rho = 1/q_{95}$, consistent with low-q H-mode data from DIII-D [10]. Note that no probability of enhanced α losses, above the usual losses of heating efficiency in the tokamak database, is assumed in these estimates, since the study of α heating efficiency, including the effects of anomalous α losses, is a major objective of the CIT experiment.

By evaluating the results of this Monte-Carlo study for a set of CIT-like devices with $R/a = 3.24$, $B_T = 9$T (for approximately fixed engineering difficulty), and $R \alpha I_p$ (for fixed q), the range of expected performance can be plotted *vs.* I_p, as shown in figure 2. As can

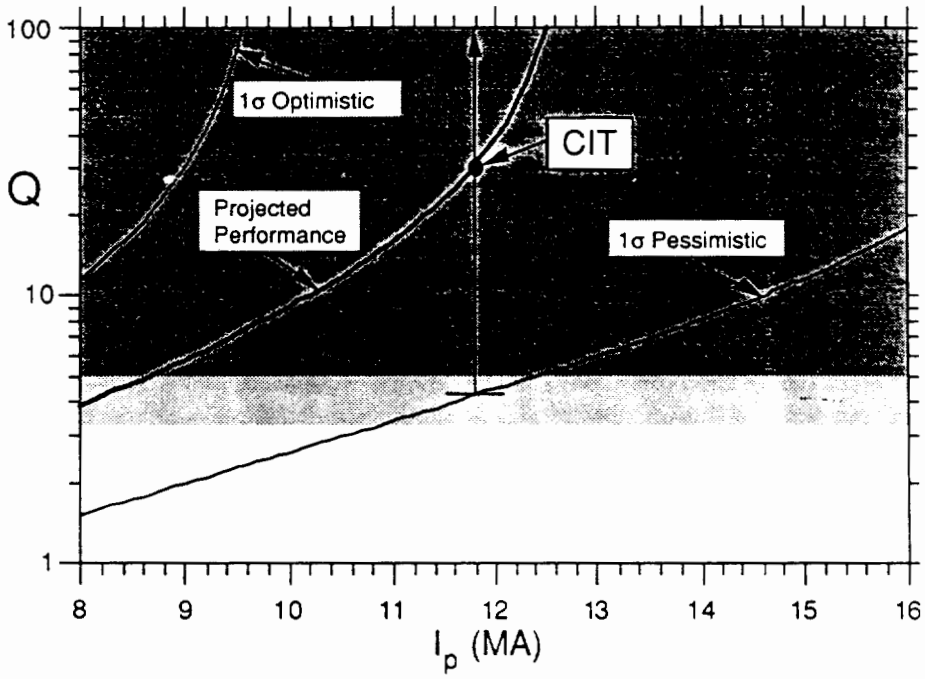

Fig. 2: Nominal, 1σ optimistic, and 1σ pessimistic projections for Q vs. plasma current, for a range of CIT-like devices with B_T = 9T, R/a = 3.24, and R α I_p. Dark shading shows region of $P_\alpha > P_{aux}$.

be seen, CIT has high confidence of reaching Q > 5, where P_α exceeds P_{aux}. Center-of-the-error-bar projection gives Q = 30, with fusion power ~ 500 MW. Under these circumstances α heating efficiency can be studied at Q > 5 over a very wide range of plasma and α-physics parameters (see fig. 4a). An identical analysis for ITER inductive long-pulse operation at 22MA, with 10% He ash accumulation and 2% C, gives the same Q = 30 as CIT at 11.8MA, with 3% He and 2% C (Z_{eff} = 1.65). Experimental operations and optimization studies on CIT thus should contribute considerably to confidence that ITER will be able to operate at the slightly above-nominal performance (by this analysis) required to attain long-pulse ignited operation. Both devices require only ~2.05x ITER89-P L-mode for ignition, under the other standard assumptions listed above.

The CIT Physics R&D Plan [11] has a strong focus on improving the ability to predict plasma performance based on extrapolating along lines of dimensionless similarity [12]. This research is being done in collaboration with the Transport Task Force, and the DIII–D and TFTR experimental teams. Preliminary results indicate that if the basic mechanisms of transport are due to instabilities with scale-size set by intensive variables (e.g. ρ_i or c/ω_p) as expected theoretically, rather than by extensive variables (e.g. R or L_n), then extrapolation from present tokamak data to CIT along the variable ρ_i/a, at fixed β and ν*, shows that CIT will easily obtain ignition. Further work is required, however, to conclusively demonstrate intensive ("gyro-Bohm") scaling. Validated, theory-based transport models will eventually be required in order to permit accurate, detailed

prediction of all aspects of plasma transport. A wide range of theoretical models are being testing against experimental data in order to work towards this goal.

α-Particle Physics

In the above analysis we have assumed classical collisional α behavior. However an increasing number of theoretical [13] and experimental [14-21] results suggesting non-classical α effects point to the importance and special interest of investigating these effects in the burning plasma state (reviewed also in [22]). α simulation experiments based on using ICRF minority heating [23] are limited to the effects of energetic trapped ions, which are not capable of exciting the parallel shear Alfvén resonance, $\omega - k_{||}v_{||} = 0$, where $\omega = k_{||}v_A$. First results using quasi-tangential neutral beam injection [20,21], despite difficulty in achieving $v_{beam} > v_A$, do suggest excitation of the Alfvén spectrum. Energetic ion losses due to these modes have been observed on TFTR. Ultimately these effects, also including α ballooning and α fishbone modes, have to be investigated in a burning plasma experiment such as CIT, where a wide parameter space can be explored and α heating efficiency can be measured quantitatively. Theoretical results of linear and finite amplitude α collective effects in CIT are described in the remainder of this section, aiming to delineate stable and unstable operating regions and to assess the impact of possible anomalous losses for CIT and for larger machines such as ITER.

General Considerations

Before going into the details of individual modes, it is valuable to asses the impact of reduced coupling of the α power ($P_{\alpha o} \equiv S_f E_{\alpha o}$, $S_f \sim (\sigma_f v) n_e^2/4$) to the background plasma. Given an anomalous D_α, and associated fast α loss frequency, $\nu_L \sim 4D_\alpha/a^2$, it follows readily from α power balance that the coupling parameter $\eta_\alpha \equiv [P_\alpha(\text{coupled})/P_{\alpha o}]$ is given by

$$\eta_\alpha = 1 - \nu_L \frac{n_\alpha \bar{E}_\alpha}{S_f E_{\alpha o}}; \quad n_\alpha \bar{E}_\alpha = \int_0^{v_{0\alpha}} d^3v \frac{m_\alpha v^2}{2} f_\alpha \tag{1}$$

and we note that in steady state $S_f/n_\alpha \sim 1/\tau_{sd}$. $n_\alpha \bar{E}_\alpha$ is the velocity distribution (f_α) averaged α pressure including the effect of ν_L on the kinetic equation for f_α. (For $\nu_L \tau_{sd}/3 \sim 1$ the slowing down distribution is strongly affected.) Given η_α, we follow a recent work of D. Cohn [24]. The bulk plasma power balance $3nT/\tau_E \equiv P_{loss} = P_{aux} + \eta_\alpha P_\alpha$ and the definition $Q \equiv 5\, P_\alpha/P_{aux}$ yields

$$Q = \frac{5P_\alpha}{P_{loss}}\left[1 - \eta_\alpha\left(\frac{P_\alpha}{P_{loss}}\right)\right]^{-1} \tag{2}$$

Defining

$$\left(n\tau_E\right)_* \equiv 12T/\left\langle\sigma_f v\right\rangle E_{\alpha o} \rightarrow \frac{P_\alpha}{P_{loss}} = \frac{n\tau_E}{\left(n\tau_E\right)_*} \tag{3}$$

Note that $(n\tau_E)_*$ is a function of temperature only and if $\eta_\alpha \equiv 1$, achieving $n\tau_E = (n\tau_E)_*$ describes ignition. We rewrite Eq. (2) as

$$Q = 5\left(\frac{n\tau_E}{(n\tau_E)_*}\right)\left[1 - \eta_\alpha \frac{n\tau_E}{(n\tau_E)_*}\right]^{-1} \tag{4}$$

and obtain Fig. 3, showing (i) how for a given normalized ignition margin $n\tau_E T/(n\tau_E)_* T$, Q drops as η_α decreases below 1, and (ii) how, for a desired Q, $(n\tau_E)/(n\tau_E)^*$ has to be increased as η_α drops. From Eqs. (1 – 4) it thus becomes apparent how collective α effects producing an anomalous D_α could impact CIT performance, and thus be detectable. The experimentally observed offset-linear dependence of plasma stored energy on heating power [25] implies that the incremental stored energy at Q = 5 operation, relative to ohmic, should be twice that achieved with RF heating alone in a non-reacting plasma. $\eta_\alpha < 1$ will be detectable as a reduced incremental confinement time, τ^{inc}, for α heating. Quantitative measurements of τ^{inc} due to α's require Q > 5.

Let us assume $D_\alpha \sim \chi_e$, consistent with theoretical estimates for α-driven ballooning modes (see below). Then it is reasonable to take $\nu_L \sim 1/\tau_E$ and to use this value in Eq. (1) for $\eta_\alpha \equiv \eta_\alpha(n, T)$, evaluated for a slowing down distribution f_α. Since the loss frequency ν_L vanishes in the α stable domain in n – T space we adopt the approximate stability boundary of the α ballooning mode [26] $\beta \sim 0.25\beta_{Troyon}$. The resulting POPCON plot of P_{aux}, Q and β_α for CIT parameters is shown in Fig. 4b and, for comparison, the $\eta_\alpha = 1$, $\nu_L = 0$ POPCON plot in Fig. 4a. Since from Eq. (1) our assumption $\nu_L \sim 1/\tau_E$, $\eta_\alpha \sim 1 - \tau_{sd}/3\tau_E \sim 0.9$ the moderate loss in fusion power output (Q = 28 → 20, P_{aux} = 16 MW → 23 MW; at <nT>/<n> = 10 keV, <n> = 3 x 10^{20} /m^3) can be easily understood (comparing Figs. 4a and 4b). From an experimental perspective, at <n> = 3 x 10^{20} /m^3, 20 MW of heating will produce <nT>/<n> = 11.2 keV for $\eta_\alpha = 1$, but only 9.4 keV with the modest α losses resulting from $\nu_L \sim 1/\tau_E$.

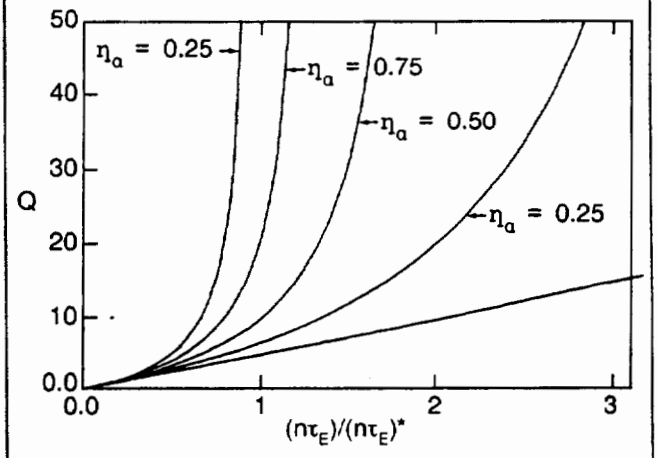

Fig. 3: Q vs. normalized ignition margin for different values of α coupling parameter, η_α, from [24]

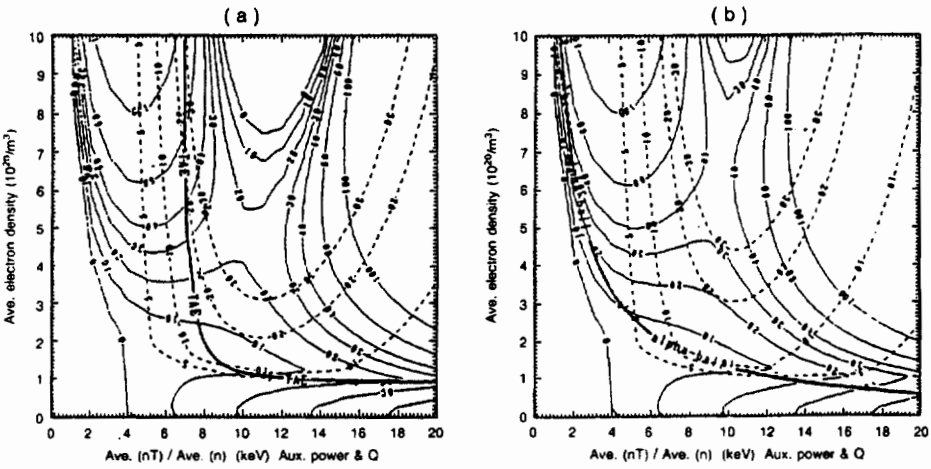

Fig. 4a, b: Plasma OPerational CONtour (POPCON) plots for CIT with 1.85xITER89-P scaling and standard profiles. Solid lines indicate required auxiliary heating power, dashed curves indicate Q. In 4a, $\eta_\alpha = 1$, and the thick curve shows the TAE threshold. In 4b the thick curve indicates the region of α-driven ballooning instability, and $\nu_L = 1/\tau_E$ is used to evaluate η_α in the region of instability.

Toroidal Alfvén Eigenmode

The linear theory of the TAE has received much attention (cf. the synopses in Refs. [13] and [22]). For the present purpose we use the work of C.Z. Cheng [27], which develops the linear theory results from the Nova-K code, describing fast α's by a slowing-down distribution. The toroidal gap mode frequency is given by

$$\omega_r = \left(\frac{v_A}{2R_0 q}\right)_{gap} \qquad q_{gap} = \frac{m+\frac{1}{2}}{n} \tag{5}$$

where (n,m) are the toroidal / poloidal mode numbers and the gap location is determined from $k_\parallel^2(m) \approx k_\parallel^2(m+1)$. The marginal stability criterion can be cast in the form (see Ref. [27], Eq. (37))

$$\beta_\alpha\left[\frac{\omega_{*\alpha}}{\omega_r} F_1\left(\frac{v_A}{v_\alpha}\right) - F_2\left(\frac{v_A}{v_\alpha}\right)\right] = \beta_e \frac{v_A}{v_{the}} \tag{6}$$

where $\omega_{*\alpha} = \left(\frac{m}{r}\right)\frac{\bar{E}_\alpha \partial n_\alpha/\partial r}{e_\alpha n_\alpha B}$ is driven by the energetic alpha density gradient and $\bar{E}_\alpha \equiv \overline{mv_\alpha^2/2}$ is the fast α energy, averaged over the α distribution function. The functions $F_{1,2}(v_A/v_\alpha)$ originate from inverse and regular Landau damping on the α's and electrons, see Ref. [27]. Equation (6) is obtained from an analytic large-aspect-ratio dispersion relation, localized in radius around the gap mode peak. The more exact marginal stability curve ob-

tained numerically with the Nova-K code from a global stability calculation is shown in Fig. 5 for CIT equilibrium parameters. In this calculation, $n_\alpha = n_\alpha(o)e^{-r^2/L_\alpha^2}$ is assumed and results are shown for $L_\alpha/a = .2$ and .3 for fixed temperature $T_{eo} = T_{io} =$ 10 and 20 keV. (a is the minor plasma radius.) In this figure, the volume averaged $<\beta_\alpha>$ and the ratio of α-birth-speed to Alfven speed v_α/v_A are free parameters entering the kinetic part of the Nova-K code, producing the Alfvén gap mode spectrum for a fixed MHD equilibrium. The toroidal mode number is fixed at n = 1, the poloidal spectrum centers about m = 1 and 2. The plasma is stable below each curve and unstable above. The sharply rising boundary on the left comes from the left hand side of (6), i.e., the condition $\omega_{*\alpha}/\omega_r > F_2/F_1$ for instability. $F_2/F_1 \sim O(1)$. By increasing $v_A \propto B/\sqrt{n_i}$ one can thus avoid instability but at B = 9 T, $v_{\alpha o} < v_A$ requires $n_i < 0.57 \times 10^{20}$ /m^3 (for a 50:50 D–T plasma) which is below the expected operating region. Concerning β_α, at fixed $\beta_{th} = 3\%$, $\beta_\alpha = 1.5 \times 10^{-4}$ at 5 keV and $\beta_\alpha = 0.01$ at 20 keV (cf. Fig. 3 of Ref. [22]). The linear stability condition Eq.(6) is violated in high temperature CIT operation, but should be stable at the lower temperatures and higher densities accessible to CIT. Experimental results from CIT investigating these effects should be of special importance to ITER engineering-phase operation, which requires very high plasma temperatures for efficient current drive, while employing super-Alfvénic parallel-moving beam ions to carry current.

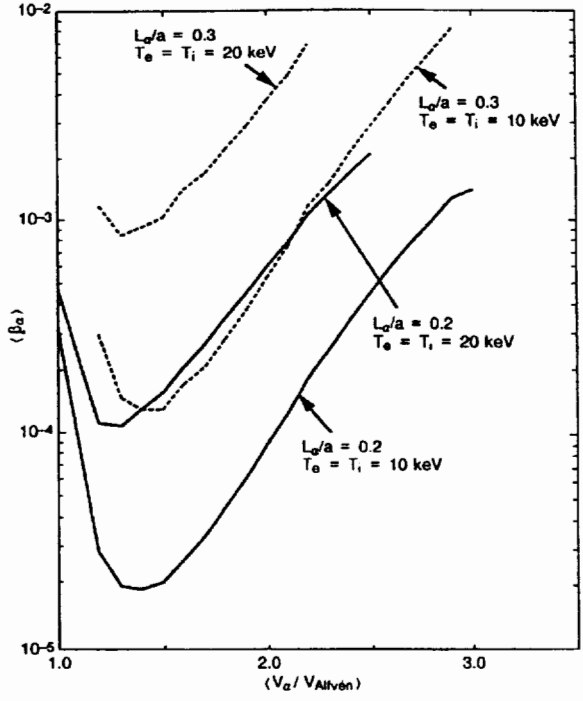

Fig. 5: Global eigenvalue calculation delineating the TAE stability boundary at fixed T for standard CIT equilibrium. L_α/a is the ratio of α density gradient scale length to minor radius [27].

Linearly, broadening of the α density is stabilizing. For typical n and T profiles $L_\alpha(\text{birth})/a \geq 0.20$. If one assumed that the nonlinear consequence of the TAE-induced anomalous α transport was to broaden $n_\alpha(r)$ until it decreased $\omega_{*\alpha}$ enough to satisfy Eq. (6) a simple estimate gives L_α (marginal)/a ~ 0.5. Such an $n_\alpha(r)$ profile implies modest changes in the α power deposition, but there is no clear reason to expect such a benign saturation mechanism, rather than, for example, the strong relaxation oscillations

observed in beam-driven fishbone modes, which can substantially deplete the beam ion population.

Besides quasilinear profile broadening and flattening of the resonance region in velocity space [28], saturation by MHD mode coupling [29] and α orbit losses due to the finite amplitude TAE waves [30] are being considered. With regard to the last, a more rigorous analysis of single α particle guiding center loss in action angle variables as well as Monte Carlo simulations of an ensemble of fast α's have been done at prescribed $\widetilde{B}_r/B_o \geq 10^{-4}$. The simulation now is arranged such that prompt loss orbits are entirely removed from re-entering the statistics. Qualitatively the earlier results of Ref. [30] are confirmed. The resonance condition $\omega - k_{||}v_{||\alpha} - k_{\perp}v_{D\alpha} = 0$ where $\omega = \omega_{gap}$ is maintained for up to 10 α transit times, during which period the particle loses energy to the wave, see Fig. 6, for realistic tokamak geometry and radial TAE mode structure. During resonance periods the α's also suffer a secular radial drift outward which scales $\propto \widetilde{B}_r/B_o$. Over longer periods they experience a random walk in constant–of–motion space $(E, \mu B_o/E, P_\phi)$ which scales $\propto \left(\widetilde{B}_r/B_o\right)^2$. Stochastic orbit overlap is expected to occur when more than one toroidal mode number is admitted. Several gap modes can indeed co-exist, semi-localized at different radii, depending on the profiles of $\omega_A^2 \equiv k_{||}^2 v_A^2$, where $R_o k_{||} = n - m/q(r)$. For example, when the ion density (contained in v_A^2) varies as $n_i \sim [q(r)]^{-2}$ a channel of frequency gaps can open from the plasma center to the edge without encountering a continuum branch near the edge (which could act as a damping mechanism [31]). Quantitative results of Monte Carlo modeling of α phase space diffusion into the prompt orbit loss region are underway. Much more work (including improvements in linear continuum mode damping, nonlinear saturation, and calculations of a self-consistent D_α) is needed before the impact on CIT can be firmly assessed.

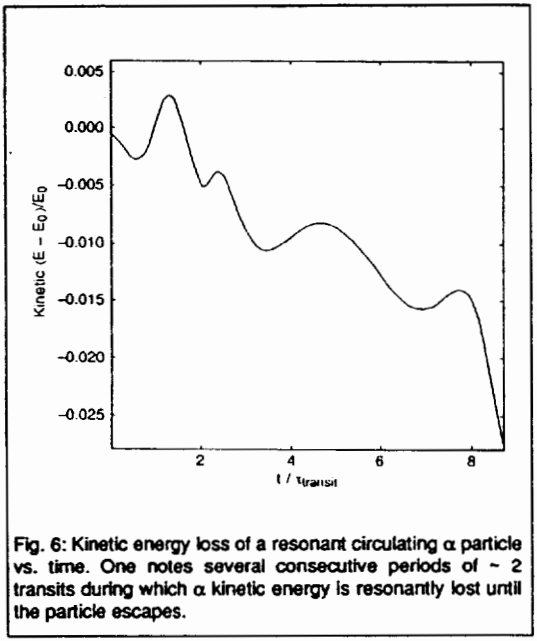

Fig. 6: Kinetic energy loss of a resonant circulating α particle vs. time. One notes several consecutive periods of ~ 2 transits during which α kinetic energy is resonantly lost until the particle escapes.

α Ballooning Modes

The standard ballooning stability threshold can be lowered by the presence of fast α's. Earlier work [32], [26] has recently been extended to a high frequency branch $\omega_r \sim \omega_A$ for high mode numbers [33,34]. The low frequency branch $\omega_r \sim \omega_{*pi}$ can be stabilized when the fast α banana precession frequency exceeds ω_r. The high frequency α-driven branch is unstable. It has a simplified (local) β_α threshold valid for $\varepsilon(v_A/v_\alpha) \geq \kappa_\theta \rho_\alpha \geq (L_\alpha/R_o q)$:

$$\beta_\alpha^{crit} \sim f_r^{-1} \frac{v_\alpha}{v_A} \left(\beta_e \frac{m_e}{m_i}\right)^{1/2}$$

where f_r is the fraction of resonant α particles. For v_α/v_A = 1.5, this gives typically $\beta_\alpha^{crit} \sim 10^{-3}$ a value easily achieved in CIT. However, this high n mode is not expected to produce a hard β limit but a soft onset of fast α diffusion. Using quasilinear theory, Rewoldt estimates in Ref. [26] that $D_\alpha \sim \chi_e$ on the ballooning unstable flux surfaces, cf. Fig. 13 of Ref. [22]. In Ref. [26] it was shown that in terms of the background β_{th}, the α ballooning threshold is exceeded for $\beta_{th} > \sim\beta_{Troyon}/4$, as indicated in Fig. 4b.

To perform a more detailed analysis for CIT, radial profiles of n, T, and q were taken from a run of the BALDUR radial transport code simulating H-mode operation in CIT. The radial density profiles for the background species are very flat in the interior, while the α–particle density profile is very steep. In addition to the ω_{*pi} root, another unstable eigenmode branch was found at higher frequency, $\omega_r \sim \omega_A >> \omega_{*pi}$, with a larger linear growth rate, which is a high-n extension of the low-n TAE. This new ω_A root is destabilized by increasing steepness of the α-particle density profile. Its growth rate peaks for $k_\theta \rho_i \sim 0.08$, n ~ 13. The real frequency is of the same order as the circulating α-particle transit frequency, so the corresponding transit frequency resonances (Landau damping or inverse damping) are strong. This $\omega_r \sim \omega_A$ root has a lower β_c than the ω_{*pi} root, but more work is required to fully understand even the linear characteristics of this mode.

Experimentally, there are three preliminary observations possibly related to $\omega \sim \omega_A$ modes destabilized by super-Alfvénic particles, Refs. [14], [20], and [21]. In DIII-D [20] the poloidal mode structure is found to have a ballooning character, and instability requires the neutral beam β to exceed a threshold substantially higher ($\beta_b \sim 2\%$) than the low mode number limit given in eq. 6. In TFTR [21] the mode phase velocity is found to scale with the Alfvén speed, and drops in neutron emission are seen in coincidence with mode activity.

Alpha Fishbone Oscillations

The linear theory and threshold calculations for α-driven fishbones have been re-addressed recently [35,36]. Following [35] the threshold value for the onset of α-driven fishbones is $\beta_{\alpha,trapped}^{crit} = \epsilon\langle\omega_{D\alpha}\rangle/\omega_A$ where $\langle\omega_{D\alpha}\rangle = v_\alpha^2 q/2rR\Omega_\alpha$, $\omega_A = v_A/\sqrt{3}R\left(rq'/q\right)_1$. Here Ω_α is the α gyrofrequency and the shear parameter $s = (rq'/q)_1$ is evaluated at the q = 1 resonant surface. s cannot be measured easily and is estimated to be s ~ .2 (depending on q(o) and $r_1/a \sim q(a)^{-1}$). This formula for β_α^{crit} was derived analytically in the limit of deeply trapped particles. Inserting the present CIT parameters yields $\beta_\alpha^{crit} \sim 10^{-2}(v_{\alpha o}/v_A)$. (For a fuller treatment of this threshold cf. Eq. (40) in Ref.[35].) For B = 9 T, n = 3 x 10^{20} /m^3 $v_{\alpha o}/v_A = 2$, and $\beta_\alpha^{crit} \sim 2\%$, which is not reachable with thermalized fusion even at T > 20 keV (see Fig. 3 of Ref. [22]). Thus CIT should be stable to α-driven fishbones unless the contributions from α pitch angles other than deeply trapped ones plays a strong destabilizing role [37].

CIT Physics Design

The detailed design of CIT is based, to the greatest extent possible, on operating conditions and techniques which have proven reliable in previous tokamaks. Nonetheless, in some areas the performance of CIT constitutes such a significant step beyond what has been achieved in previous devices that modeling studies must be used to make the necessary extrapolation from the current data base. Two especially important areas are disruptions and power handling. The CIT physics analyses in these areas are reviewed below.

Disruptions

Major plasma current disruptions are anticipated in CIT, even though the nominal plasma parameters lie well within expected stable operating boundaries. The device design assumes 10% disruptivity in all modes of operation. Time-dependent, axisymmetric analysis of disruptions is performed using the Tokamak Simulation Code (TSC), which self-consistently models plasma equilibrium and currents in the coils, vacuum vessel, and structural components. It also takes into account "halo" currents which flow through the plasma scrapeoff layer and into the vessel and internal components. Results from TSC provide the input for non-axisymmetric electromagnetic models used to determine the detailed force loads on the tokamak vacuum vessel and internal components.

Based on extrapolations from tokamak data, projected disruptions in CIT are characterized in terms of: 1) a thermal-energy quench time $\leq$1 ms, 2) a current decay rate of up to 3 MA/ms, 3) radial and vertical drifts consistent with the changes in the equilibrium profiles, current, and external field, and 4) halo currents of 10 – 20% of the initial toroidal plasma current. A range of disruption scenarios is examined in an effort to determine credible "worst case" structural loads.

In highly elongated tokamaks fast vertical disruptions, or "Vertical Displacement Events (VDE's)," can be dangerous, having caused large structural loads in JET, DIII–D, and PBX–M. Examination of the magnetic data from these events has shown that substantial halo currents flow in a wide plasma scrape-off region during both the drift phase and the current quench phase of the VDE. The vacuum vessel provides a return path for these currents, which are superimposed on the induced eddy currents already present in the vacuum vessel. The electromagnetic load distributions on the vacuum vessel are significantly altered as a result. Moreover, since the halo currents pass through the first wall components, the IxB forces due to the halo currents must be taken into account in the structural design of these components as well.

Experimentally, a VDE is precipitated by the loss of vertical control, due to a change in profiles or a shift of the plasma to a region of unstable field curvature. This is simulated in TSC as an external field perturbation combined with a disabling of the feedback control system. The plasma begins to drift vertically, with little or no loss of current; as it drifts, the cross section shrinks, q_ψ decreases, and halo currents begin to flow. The halo region is reasonably well modeled by a radial width corresponding to 40% of the initial plasma

poloidal flux, and a resistivity corresponding to a plasma temperature in the range of 4 – 40 eV. The plasma current is everywhere parallel to the magnetic field in this low pressure region. The current quench phase of the VDE is initiated when q_ψ at the 95% flux surface reaches ~ 2, at which time the plasma has drifted ~ 0.5m from the tokamak midplane. Measurements on DIII–D show poloidal halo currents up to 20% of the initial toroidal plasma current. These currents are measured both during the drift and the current-quench phases. The halo parameters in TSC are modeled on the basis of this behavior. Interestingly, the presence of the halo currents slows the vertical drift of the plasma in the simulations, as observed in experiment. Figure 7 displays the time history in TSC of toroidal plasma and vacuum vessel current, halo current, and the resulting electromagnetic pressure on the inboard surface of the vacuum vessel. In this example the plasma drifted 0.6m from the midplane in ~ 280 msec before disrupting. To safely withstand the high peak forces (equivalent to ~ 35 atmospheres) seen in the worst disruption scenarios, this region of the vacuum vessel is constructed of high-strength alloy steel (Inconel 625), with a thickness of ~ 7 cm.

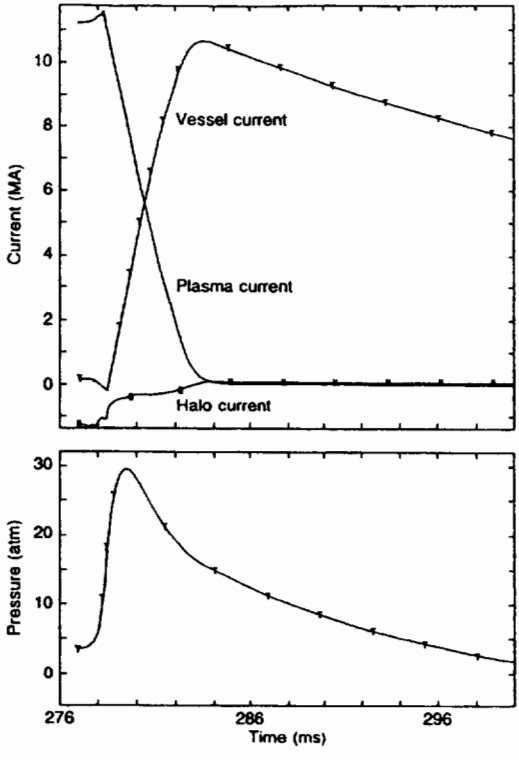

Fig. 7: Toroidal plasma and vacuum vessel currents, poloidal halo current, and average pressure on the vacuum vessel inner wall *vs.* time during a VDE disruption in CIT.

Power Handling

Under burning-plasma conditions in CIT, up to 100 MW of thermal power (from α plus auxiliary heating) must be exhausted through approximately 100 m^2 of plasma surface area. The surface-average heat flux of ~ 1 MW/m^2 is characteristic of what will be desirable in an economic fusion reactor. In the divertor configuration this heat flux is strongly peaked near the intersection of the separatrices and the divertor target plates, and so constitutes a major engineering-physics challenge for CIT, ITER and future reactors. To minimize the impact on plasma performance due to fuel dilution by impurities and due to bremsstrahlung radiation, low Z_{eff} (~ 1.65) is required. This is reflected in the CIT design in the use of high plasma densities and low–Z first wall materials, operated at a pre-shot temperature of 350°C.

The relatively short pulse length required to study α heating efficiency permits the use of a passive heat removal system employing high-thermal-conductivity graphite divertor plates. The separatrices are swept poloidally across a ~ 20 cm wide area (fig. 8) to maintain a surface temperature less than 1700°C, since TFTR [38] shows sharp increases in carbon influx above temperatures in that range, consistent with the expected effect of radiation-enhanced sublimation.

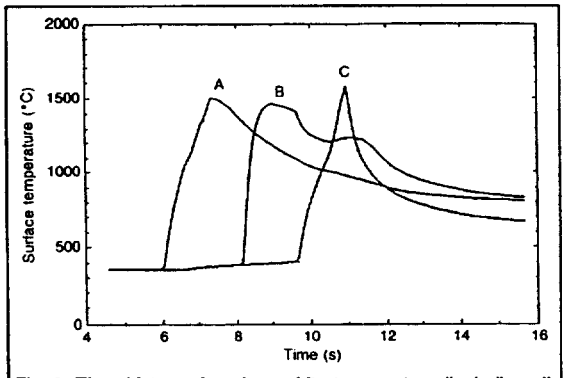

Fig. 8: Time history of peak graphite temperature (including all asymmetries) at three points along the divertor plate.

Estimates of the target heat flux densities depend on a number of factors: 1) the fraction of power lost through radiation, 2) plasma transport in the divertor channels just outside of the separatrix, 3) magnetic and component geometry in the X–point region, and 4) up-down, in-out, and toroidal asymmetries. Guidelines for these factors in CIT are based conservatively on experimental results where they are available. For power-handling purposes, it is assumed that only 40% of the power is lost through radiation – 20% in the form of core bremsstrahlung, and 20% as edge and divertor line radiation. The energy e–folding width at the outboard midplane, λ_q, is estimated to be ~ 5 mm, based on two-dimensional edge modeling (using the Braams B2 code [39]) with perpendicular heat diffusivities χ_i = 1 m²/s, χ_e = 3 m²/s, consistent with DIII–D experimental results [40]. The energy e-folding distance increases to ~ 5 cm at the divertor plate, due to expansion of the magnetic flux surfaces. The swept divertor makes the uncertain scrape-off width a much less critical parameter for CIT than for an equivalent static configuration. The exact time-varying magnetic geometry of the divertor is obtained from TSC discharge simulations. The X–point remains at least 10 cm from the inner divertor strike point and at least 15 cm from the outer strike point throughout the sweep. DIII–D measurements [41] show that up-down asymmetries of 1.2:1 in the total heat loads can be maintained by careful vertical position control. In-out asymmetries of ~ 1:4 are observed in DIII–D, PDX [42], and ASDEX data. Using these results as guidelines, 100 MW of power loss results in a maximum of 26 MW to either of the outer target plates. Allowing for a toroidal peak-to-average asymmetry of 1.5:1, which can be achieved through the use of a new "sawtooth" tile configuration (to eliminate exposed leading edges) and rigorous control of field errors, the instantaneous peak local heat fluxes are projected be in the range of 50–70 MW/m². The effects of these high heat fluxes are mitigated by the swept-divertor operation, such that the heat source passes over a given spot on the divertor surface in a short time (fig. 8), and thus the graphite temperature never exceeds 1700°C at any location.

The calculated divertor power handling capability permits a 3 s flat-top ignited burn at 500 MW of fusion power, or 10 s flat-top operation at Q = 5, with 100 MW of fusion power, in addition to a 3 s power rise time and 2 s fall time in both cases. Inner-wall limiter discharges can sustain similar power loads. Estimates of the net erosion for the divertor conditions, obtained using the REDEP [43] code, are < 3000Å per shot, or < 1 mm for the lifetime of the machine. Even with a conservative estimate for T_e at the strike point (65 eV), the erosion is found to be limited because of: 1) the short pulse length, 2) the divertor sweep, 3) the high calculated plasma density (7×10^{20} /m^3) in front of the divertor plates (giving a short mean free path for eroded carbon), and 4) the field line geometry with B_p nearly perpendicular to the divertor plates. Further self-consistent analysis (e.g. including radiation in the divertor channels) is required for a more confident assessment of divertor erosion rates.

The divertor material ablation depth due to disruptions is estimated to be less than 1mm per disruption, at the separatrix strike point. This implies that the plate lifetime will not be limited by disruptions, assuming a reasonable scatter over the swept area.

Conclusions

CIT is a key element in the world fusion program. It is designed as a burning plasma physics experiment, optimized to provide critical information about the physics of self-heated fusion plasmas, at minimum risk and cost. CIT will also enhance confidence that ITER will be able to meet its mission as an Engineering Test Facility, by providing valuable information for the final design and construction of internal components and external subsystems, and by providing early operating experience with self-heated, DT plasmas.

The CIT design provides high confidence of being able to investigate α heating efficiency over a wide range of plasma parameters. The physical phenomena associated with α heating may prove to be complex, and the ability to operate in both stable and unstable parameter regions is crucial. At this time the anticipated α-driven instabilities in CIT are the TAE modes at low and high n, and the α-driven ballooning modes. The most dangerous α particles for destabilizing these modes appear to be those with high parallel velocities. Experiments on CIT will explore α-driven instabilities over a wide range of parameter space, and quantitatively determine their effect on α heating efficiency.

The engineering-physics issues for CIT are similar to those for ITER. Present analyses indicate that disruptions and power-handling will be manageable for CIT, but experience in these areas on CIT should be of great value to ITER and devices beyond.

REFERENCES

[1] CIT General Requirements Document, W-890308-PPL-01, updated September 1990.

[2] BROMBERG, L., et al., (Proc. 10th Symposium on Fusion Eng., Phila., 1983)181.

[3] PARKER, R.R., et al., in 12th Intl. Conf. on Plasma Physics and Cont. Nucl. Fus., Nice, (1989) Vol. 3, 341.

[4] KADOMTSEV, B.B., Sov. J. Plasma Phys. 1 (1975) 295.
[5] YUSHMANOV, P. et al., Nuclear Fusion 30(1990) 1999.
[6] RIEDEL, K.I, Private communication, August 1990; "On Dimensionally Correct Power Law Scaling Expressions for L Mode Confinement," submitted to Nuclear Fusion.
[7] CORDEY, J., et al., IAEA-CN-53/F-3-19, this conference.
[8] GOLDSTON, R.J. et al., in 17th EPS Conference on Cont. Fus. and Plasma Heating, Amsterdam, (1990) Vol. 1, 134.; S. Ho, J. Perkins, Nucl. Fus. 29 (1989) 81.
[9] BUSH, C.E., et al., IAEA-CN-53/A-4-5, this conference.
[10] KELLMAN, A., private communication, 1990.
[11] CIT Physics R&D Plan, AE-900216-PPL-01.
[12] WALTZ, R.E., et al., IAEA-CN-53/D-4-7 and Ref. [11].
[13] KOLESNICHENKO, Y., SIGMAR, D., Nucl. Fus. 30 (1990) 777.
[14] LEONOV, V., MEREZHKIN, V., MUKHOVATOV, V., et. al., in 8th Intl. Conf. on Plasma Physics and Cont. Nucl. Fus., Brussels, (1981) IAEA-CN-38/N-2, Vol. I, 393.
[15] HEIDBRINK, W.W., HAY, R., STRACHAN, J.D., Phys. Rev. Lett. 53 (1984) 1905.
[16] HEIDBRINK, W.W., BEIERSDORFER, P., Nucl. Fus. 27 (1987) 608.
[17] LOVBERG, J., HEIDBRINK, W.W., STRACHAN, J.D., et al., Phys. Fluids B 1 (1989) 874.
[18] HEIDBRINK, W. W., SAGER, G., Nucl. Fus. 30 (1990) 1015.
[19] ZWEBEN, S.J., et al., Nucl. Fus. 30 (1990) 1551.
[20] HEIDBRINK, W.W., on DIII-D, private communication, 1990; submitted to Nuclear Fusion.
[21] WONG, K.L., on TFTR, private communication, 1990.
[22] FURTH, H.P., GOLDSTON, R.J., ZWEBEN, S.J., SIGMAR, D., Nucl. Fus. 30 (1990) 1799.
[23] BICKERTON, R., et al., in 12th Int. Conf. on Plasma Physics and Cont. Nucl. Fus., Nice, (1989) IAEA-CN-50/A-I-3, Vol. I, 41.
[24] COHN, D.R., MIT Report PFC/JA-9-6, submitted to J. Fusion Energy, 1990.
[25] BELL, M. et al., Plasma Physics and Cont. Fus. 28 (1986) 1329.
[26] REWOLDT, G., Phys Fluids 31 (1988) 3727.
[27] CHENG, C.Z., PPPL Report 2717 (July 1990), to be submitted to Phys. Fluids.
[28] BERK, H., BREIZMAN, B., Phys. Fluids B 2 (1990) 2246 .
[29] CARRERAS, B., et al., private communication, 1990.
[30] SIGMAR, D., HSU, C.T., CHENG, C.Z., WHITE, R.E., MIT Report PFC/KA-89-8 and Ref. [13].
[31] VAN DAM, J., in IAEA-CN-53/D-3-6, this conference.
[32] SPONG, D., SIGMAR, D., et al., Phys. Fluids 28 (1985) 2494.
[33] SPONG, D., et al., Kiev Conf. op. cit. in [13], to be published in Fus. Techn. 1990.
[34] FU. G.Y., CHENG, C.Z., Phys. Fluids B 2 (1990) 985.
[35] WHITE, R.E., ROMANELLI, F., BUSSAC, M., Phys. Fluids 32 (1990) 745.
[36] COPPI, B., MIGLIUOLO, F., et al., Phys. Fluids B 2 (1990) 927.
[37] CHENG, C.Z., IAEA-CN-53/D-3-6, this conference.
[38] ULRICKSON, M., Presented at the 9th International Conference on Plasma Surface Interactions, Bournemouth. UK, to be published in Journal of Nuclear Materials.
[39] BRAAMS, B.J., SINGER, C.E., Fusion Techn. 9 (1986) 320.
[40] HILL, D.N., et al., General Atomics Report GA-A20138 (1990) to be published in J. Nucl. Mater.
[41] HILL, D.N., et al., General Atomics Report GA-C19927 (1989).
[42] FONCK, R.J., et al., J. Nucl. Mater. 111 & 112 (1982) 343.
[43] BROOKS, J.N., Journal of Nucl. Mat. 170 (1990) 164 - 168.

DISCUSSION

S.A. COHEN: What is the likelihood that CIT will have H mode confinement, considering that experiments such as JET and DIII-D show a power threshold that increases with toroidal field?

D.J. SIGMAR: From examining the world database on H mode thresholds, we had concluded that about 12 MW of heating power would be needed to obtain the H mode on CIT. The JET results with ICRF nicely confirm this. CIT will be equipped with 20 MW of ICRF at first, and this system will be upgradable, so we are confident that CIT will achieve H mode performance. The very latest JET results with pellets plus ICRF in the H mode — where they obtained peaked density profiles as well in a CIT-like scenario — are especially encouraging.

J.G. CORDEY: What aspects of α particle physics cannot be tested on the big machines JET and TFTR when operating in D–T? Since $\tau_{\text{slowing }\alpha} \sim \tau_{\text{energy}}$ in JET, that will be a more stringent test of α particle confinement than CIT.

D.J. SIGMAR: Many of the α particle instabilities I have discussed may be observable on JET and TFTR, and the effects on the α distribution could be severe, as you say. CIT, however, will have a much larger operational space in which to investigate these instabilities and find their thresholds, non-linear development and consequences for α and thermal transport. In addition, the ratio of α gyroradius to system size is a key parameter in, for example, the TAE mode, and TFTR and JET will not approximate a reactor in this respect. Finally, and most importantly, unlike TFTR and JET, CIT will be able to make quantitative measurements of α heating efficiency in stable and unstable regimes. At $Q \sim 1$ this is not possible. The results of the studies on CIT could have a significant impact on ITER's operational scenarios, and so affect choices in ITER's internal hardware or current drive and heating systems.

B. COPPI: Concerning the TAE modes that you discussed, my feeling and that of other colleagues is that their effects should not be too deleterious. In addition, compact high field experiments, such as Ignitor, can be designed to operate in regimes where the known forms of these modes remain stable. On the other hand, the possible excitation of fishbone modes deserves closer attention. According to our theory the relevant threshold should be more severe than the one you indicated in your figure. How did you evaluate this?

D.J. SIGMAR: The toroidal Alfvén eigenmode has been shown[1] to have a fast growth rate of $\gamma/\omega_A = 2.5 \times 10^{-2}$, and C.Z. Cheng has verified instability for CIT and ITER using the Nova-K code[2].

One can avoid the unstable region by going to $v_{\alpha 0}/v_A < 1$, see Fig. 5 in this paper. However, even at B = 12 T, this would require $n_i < 1.6 \times 10^{20}$ m^{-3}, which may be too low for an Ignitor.

The fishbone threshold was taken from Eq. (40) of Ref. [35] of the present paper; for CIT parameters this yields $\beta_\alpha^{\text{crit}} \sim 10^{-2}(v_{\alpha 0}/v_A)$, i.e. >1%, which is not easily reached. (This formula assumed $(rq'/q)|_{q=1} = 0.2$. Thus for less shear $\beta_\alpha^{\text{crit}}$ would be less.)

---

[1] For example, FU and VAN DAM, Phys. Fluids B **1** (1990) 1949.

[2] CHENG, C.Z., et al., IAEA-CN-53/D-III-6, these Proceedings, Vol. 2.